Neural Network-Based Adaptive Feedback Linearization Control of Antilock Braking System

Samuel John[1] **and Jimoh O. Pedro**[2]

[1]Department of Mechanical Engineering
The Polytechnic of Namibia
13 Storch St., Windhoek, Namibia
sjohn@polytechnic.edu.na

[2]School of Mechanical, Industrial and Aeronautical Engineering,
University of the Witwatersrand, Johannesburg,
Wits 2050, Johannesburg, South Africa
jimoh.pedro@wits.ac.za

ABSTRACT

Safety systems in road vehicles are categorised into two main types: passive and active systems. The antilock braking system (ABS) is an active safety system in road vehicles, which senses the slip value between the tyre and the road and uses these values to determine the optimum braking force. Due to the high non-linearity of the tyre and road interaction, and uncertainties from vehicle dynamics, standard control methods: like PID, sliding mode control and feedback linearization will not suffice. This paper, therefore proposes a neural network-based feedback linearization control design method. The experimental results reveal that slip regulation using neural network-based control scheme is feasible for different slip values (road conditions) and robust to external disturbances.

Keywords: Antilock braking system, slip control, neural network, feedback linearization, friction model.

2000 Mathematics Subject Classification: 93C10, 93C40, 93C85.

1   Introduction

Current antilock braking systems (ABS) research is based on slip control. The aim of the controller is to continuously monitor the slip value (λ) and by manipulating the braking pressure P_b, it is possible to avoid a slip value of 100% (wheel lock) and maintain the slip at about the desired (λ_d) value, which is estimated for most road conditions to be about 20% (Chikhi, El Hadri and Cadiou, 2005; Xu, Cheng, Sha, Ting and Ding, 2009). Since it is difficult to measure the slip (λ) directly, an estimator (or observer) is usually employed for the estimation of (λ) using the vehicle speed (v) and the wheel speed (ω). The major challenge of the slip control is the non-linearity introduced by the tyre/road interaction. Non-linear systems do not have standard methods of analysis unlike linear systems, that are analysed using the time domain or the

frequency domain. Some non-linear ABS control methods and some neural network-based approaches found in literature will be discussed. Three important non-linear control methods applied to ABS are the backstepping, sliding mode and feedback linearization control methods.

(Lin and Ting, 2007) proposes a backstepping control design scheme for a non-linear ABS assisted with active suspension system (ASS) to further reduce vehicle braking time and stopping distance. The goal is to utilise the vertical normal force that increases during braking, leading to increased frictional forces between the tyre and the road to achieve more shorter stopping distance than using just ABS. Simulation results using a quarter-car model show that the integrated system achieved a 12% improvement in stopping distance.

The feedback linearisation control (FBL) method as applied to non-linear systems is one method to turn to for solving the slip control problem. However, there exists minimum literature on the application of feedback linearisation control method to ABS. (Park and Lim, 2008) presented simulation results of a wheel slip control employing the feedback linearisation control method with an adaptive sliding mode control. The novelty of this work is the introduction of a time delay to the input. The time delay is necessary because in practice, there exists a time delay in the actuator dynamics. To compensate for the time delay, the sliding mode controller is incorporated to bound the uncertainties, using a method proposed by (Shin, Choi and Lim, 2006). The simulation results presented did not show a significant difference between the model incorporating time delay to the model without the time delay. The FBL scheme is more robust with respect to un-modelled dynamics compared to the *proportional-integral-derivative* (PID) and *sliding mode control* SMC methods. To get maximum benefit with respect to accurate slip tracking using PID and SMC, which is necessary for effective ABS performance, requires a comprehensive mathematical model. Further improved performance of the ABS can be achieved using intelligent control schemes.

With the changes in technology, there is the need to design systems to maintain acceptable performance levels in the face of significant uncertainties. Recent approaches to this problem have been the development of control system schemes that emulate intelligent biological systems. Computational intelligent methods such as neural networks, fuzzy logic, evolutionary algorithms and machine learning have been incorporated into control systems design to ensure more robust systems. The ability of intelligent systems to adapt well even when the mathematical model is not accurate enough is a good reason for employing intelligent schemes. Due to the difficulty involved in developing a mathematical model that will capture all possible vehicle braking dynamics some researchers are turning to intelligent control methods for the development of ABS controllers (Poursamad, 2009; Hsu, Lee, Hsu and Lin, 2008; Lin and Hsu, 2003).

An adaptive radial function neural network-based hybrid controller for anti-lock braking systems is proposed by (Poursamad, 2009). The hybrid controller is based on the non-linear feedback linearization method, combined with two radial basis neural network functions that are used to learn the non-linearities of the ABS. The neural network weight adaptation law used, is the

backpropagation algorithm. An on-line weight adaptation is used and the Lyapunov stability criterion was applied to study the stability of the proposed controller. Simulations are conducted to show the effectiveness of the proposed controller under various road conditions and parameter uncertainties. The author concluded that the proposed controller is more effective and superior than the standard feedback linearization control method. It is further concluded that the robustness of the NN-based hybrid controller to external disturbance, measurement noise and changes in initial conditions is more favourable than the standard feedback linearization control.

The fuzzy logic application to slip control has received a lot of attention. The fuzzy logic controller has several advantages: it can easily adapt to complex changes in the vehicle operating condition and the non-linearity of the vehicle tyre and suspension systems which gives it a good robust performance. (Yu, Feng and Li, 2002) developed a fuzzy logic controller with the objective of tracking an optimal slip ratio in real time, in order to obtain a shorter stopping distance while enhancing side slip stability. The fuzzy logic controller consisted of 25 fuzzy rules and triangular membership functions were employed. From the simulation results presented, the proposed controller was found robust because it was able to adapt to changes in road conditions. It further shortens the stopping distance by 15% compared to a controller with a fixed slip ratio scheme.

In another work, (Mirzaei, Moallem, Dehkordi and Fahimi, 2006) developed an optimal fuzzy controller for the ABS. The fuzzy membership functions and rules were of the Takagi-Sugeno-Kang (TSK) type. These were optimized using genetic algorithms and an error-based optimization techniques. The objective was to maintain a desired wheel slip value, to obtain maximum traction forces on the wheels and maximum vehicle deceleration. The error-based optimization technique was then used to get a faster convergence of the slip. The performance of the controller was tested on a vehicle model incorporating the hydraulic dynamic and also considering the dynamic load transfer from the rear to the front axle. Simulations were conducted on alternating dry-asphalt and icy-asphalt road surface. Initial vehicle speed of $30m/s$ $(108km/h)$ was used. The stopping distance was $20m$ less than the stopping distance with lock-up wheels.

In a laboratory ABS test rig, (Precup, Spataru, Petriu, Preitl, Radac and Dragos, 2010) implemented four Takagi-Sugeno fuzzy controllers (T-S FCs), employing parallel distributed compensation (PDC) method. This method is proposed by (Wang, Tanaka and Griffin, 1995) for obtaining the state feedback gain matrices. Two controllers were designed to guarantee global stability while the other two controllers were designed using the linear-quadratic regulator (LQR) technique. The main advantage of this approach is the relative simple design and low cost of implementation of the Takagi-Sugeno fuzzy controllers. The drawbacks of the method is that, only two of the four Takagi-Sugeno fuzzy controllers provide near optimum results, around an operating point. The disadvantage of this result is that it would not be able to handle the so called "split-μ" braking condition.

Artificial neural networks have been applied to different prediction problems, for example Vassileiou et al studied radial basis function networks (RBF) and multilayer perceptrons networks (MLP) for the estimation of fluid flow estimation for use in the modelling of soil erosion. The aim of the research was to develop a simple method of flow values estimation on the basis of general precipitation data. The study results indicated the feasibility of neural networks application for flow values estimation, with a preference for MLP networks, instead of simple statistical regional relationships (Vassileiou, Maris, Kitikidou and Angelidis, 2012) .

The current work proposes a multi-layered neural network-based feedback linearization (NNFBL) control scheme for tracking a pre-determined slip ratio. The NNFBL is also referred to in the literature as the *Non-linear Autoregressive-Moving Average* abbreviated as NARMA-L2 (Norgaard, Ravn, Poulsen and Hansen, 2003; Awwad, Abu-Rub and Toliyat, 2008; Adaryani and Afrakhte, 2011). The motivation for the neural network approach to the slip control design, is based on the fact that there is high uncertainty associated with the estimation of the slip (λ). This is further compounded with the possible sudden changes in road conditions. The novelty of this approach is in its ability to specifically improve the applied braking torque and its robustness to varying slip values, which relates to split μ road condition.

2   Dynamic ABS Model Formulation

The free-body diagram of a quarter-car model shown in Figure 1, is used to develop the vehicle longitudinal braking dynamics. It is made-up of a single wheel carrying a quarter-mass m of the vehicle and at any given time t, the vehicle is moving with a longitudinal velocity $v(t)$. The wheel rotates with an initial angular velocity of $\omega(t)$, driven by the mass m in the direction of the longitudinal motion. The friction between the tyre and the road surface, generates a tractive force F_x. When the driver applies the brakes, a torque is applied to the wheel and it will cause it to decelerate until it comes to a stop.
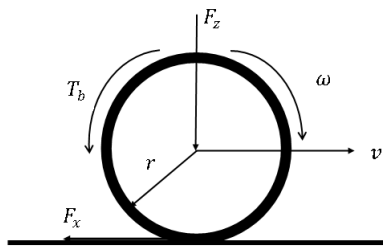

Figure 1: Quarter-car model

Applying Newton's second law of motion to the wheel, the equations describing the vehicle, tyre and road interaction dynamics during braking are developed. The equation describing the wheel rotational dynamics is given by:

$$\dot{\omega} = \frac{1}{J}(r\mu(\lambda)F_z - B\omega - T_b(sign(\omega))) \tag{2.1}$$

where J is the rotational inertia of the wheel, r is the radius of the tyre, B is the viscous friction

coefficient of the wheel bearings and T_b is the effective braking torque, which is dependent on the direction of the angular velocity.

The equation describing the vehicle longitudinal dynamics is given by:

$$\dot{v} = -\frac{1}{m}(\mu(\lambda)F_z + Cv^2) \tag{2.2}$$

where C is the vehicle's aerodynamic friction coefficient, μ is the longitudinal friction coefficient between the tyre and the road surface, λ is the longitudinal tyre slip and F_z is the normal force exerted on the wheel.

The friction coefficient between the road and the tyre relates to the slip and has significant impact on the braking of the vehicle. A simple but practical equation used to determine λ is given by:

$$\lambda = \frac{v - r\omega}{v} \tag{2.3}$$

The frictional force developed between the tyre and the road surface is the major contributor to the non-linearity of the dynamics of the ABS system. Several friction models are used for the estimation of these forces in the literature, and to describe the $\mu - \lambda$ relationship for different road conditions. The famous of these models is the *magic formulae* which has attracted a lot of research work (Bakker, Pacejka and Lidner, 1989; Pacejka and Bakker, 1993; Oosten and Bakker, 1993; Lidner, 1993). Similar graphs generated using the magic formulae are shown in Figure 2. The physics involved in the modelling of the rolling phenomenon is complex. (Bakker et al., 1989) and (Zanten, Erhardt and Lutz, 1990) in their various works provided clarification on the role of the *"wheel slip"* parameter λ. The *wheel slip* was found to be a critical parameter on which the available maximal friction coefficient depends (Corno, Savaresi and Balas, 2009).
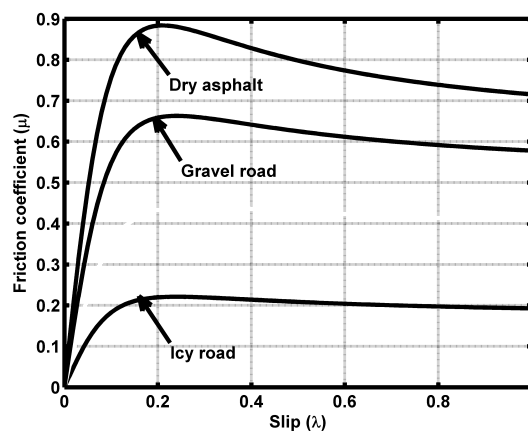

Figure 2: $\mu - \lambda$ Curves for different road conditions

The wheel slip dynamics is obtained by taking the derivative of the longitudinal wheel slip

(Equation 2.3) with respect to time, assuming that the radius of the tyre remains constant.

$$\frac{d\lambda}{dt} = \frac{\partial\lambda}{\partial v}\frac{dv}{dt} + \frac{\partial\lambda}{\partial\omega}\frac{d\omega}{dt} + \frac{\partial\lambda}{\partial r}\frac{dr}{dt}$$ (2.4)

$$\dot{\lambda} = \frac{\omega r}{v^2}\dot{v} - \frac{r}{v}\dot{\omega}$$ (2.5)

Substituting (2.1) and (2.2) into (2.5) yields the following:

$$\dot{\lambda} = -\frac{r}{v}\left(\frac{rF_x - T_b}{J}\right) - \frac{\omega r}{v^2}\left(\frac{F_x}{m}\right)$$ (2.6)

Rearranging (2.6) and knowing that $F_x = \mu F_z(\lambda, \mu_0)$ yields the slip dynamics as

$$\dot{\lambda} = -\frac{1}{v}\left(\frac{\omega}{mv} + \frac{r^2}{J}\right)\mu F_z(\lambda, \mu_0) + \frac{r}{Jv}T_b$$ (2.7)

Equation (2.7) can be described as a single-input single-output (SISO) affine system, which is given in the canonical form as:

$$\dot{\mathbf{x}} = f(\mathbf{x}) + g(\mathbf{x})u$$ (2.8)

$$y = h(\mathbf{x})$$ (2.9)

where the state variables $\mathbf{x} = [x_1, x_2]^T$ are the wheel angular velocity ω and the vehicle longitudinal velocity v respectively, $f, g : \mathbb{R}^n \to \mathbb{R}^n$ are smooth functions and y is the output slip function.

For the ABS case therefore: $f(x) = -\frac{1}{v}\left(\frac{\omega}{mv} + \frac{r^2}{J}\right)\mu F_z(\lambda, \mu_0)$, $g(x) = \frac{r}{Jx_2}$ and $u = T_b$. Note that $f(\cdot)$ and $g(\cdot)$ are non-linear dynamic functions and the goal of the ABS is to track a predetermined slip set-point (λ_d). However, some of these parameters could be perturbed, and the model may not be able to handle the internal and external disturbances. Secondly, the functions $f(\cdot)$, $g(\cdot)$ and $h(\cdot)$ may be either partially known or completely unknown (Yeşildirek and Lewis, 2001; Behera and Kar, 2009). In the case of any unknown function, neural networks could be employed to estimate the unknown function or functions. The controller parameters are therefore up-dated to achieve convergence of the error to zero, by the selection of an appropriate learning algorithm. The current work assumes that both functions $f(\cdot)$ and $g(\cdot)$ are unknown. On the basis of this assumption therefore, an indirect adaptive control method, using neural network-based feedback linearization (NNFBL) model is chosen to estimate the ABS model.

3 Description of the Laboratory ABS

The INTECO ABS laboratory system used for this work is shown in Figure 3, (Manual, 2009). It is made up of two rolling wheels; the lower wheel represents the vehicle motion while the upper wheel represents the wheel motion. Two identical encoders are used to measure the wheel and vehicle rotational motions. The accuracy of measurement of the encoders is 2048 encoder

counts per revolution, yielding $2\pi/2048 = 0.175^0$ per encoder count. Pulse width modulator (PWM) controlled DC motor of about $220W$ accelerates the lower wheel, the upper follower wheel also gains speed. The angular velocities of the wheels are estimated by differential quotients. The vehicle velocity is estimated by multiplying the angular velocity of the lower wheel ω_2 with its radius r_2, while the wheel velocity is estimated by multiplying the angular velocity of the upper wheel ω_1 with its radius r_1. When a pre-determined speed threshold value is reached, the power supply to the DC motor attached to the lower wheel cuts-off and the braking process is initiated. The braking is accomplished via a Shimano BR-M486 hydraulic braking system, used in bicycles. It consists of a thin disc and brake-pads arrangement, and has a cable wound on the shaft of the small PWM controlled DC motor and attached to the brake lever that transmits the braking torque to the upper wheel upon braking. Both DC motors are controlled by $3.5kHz$ frequency signals. The non-linear friction curve is generated by the contacting surfaces of the lower steel wheel and the upper plastic wheel.

Figure 3: INTECO ABS physical model

The friction model supplied by INTECO (Manual, 2009) is used for the estimation of the friction coefficient and it is given by Equation (3.1)

$$\mu(\lambda) = \frac{c_4 \lambda^p}{a + \lambda^p} + c_3 \lambda^3 + c_2 \lambda^2 + c_1 \lambda \tag{3.1}$$

Table 1 presents the parameters and the numerical values for the laboratory ABS test rig.

4 Neural Network-Based Controller Design

This work proposes the application of NNFBL control method. To illustrate the advantage of using NNFBL: if the nominal condition for the non-linear functions $f(\cdot)$ and $g(\cdot)$ are known, then it will be necessary to separate the known from the unknown portions of the dynamics. If for example the nominal dynamics are represented by Equation (4.1)

$$\dot{\lambda} = \mathbf{f}(\mathbf{x}) + \mathbf{g}(\mathbf{x})\mathbf{u} \tag{4.1}$$

Table 1: Experimental system parameters and numerical values

Symbol	Description	Value	Unit
r_1	Radius of the upper wheel	0.0995	m
r_2	Radius of the lower wheel	0.0990	m
J_1	Moment of inertia for the upper wheel	0.00753	kgm^2
J_2	Moment of inertia for the lower wheel	0.0256	kgm^2
M_1	Static friction of the upper wheel	0.0032	Nm
M_2	Static friction of the lower wheel	0.0925	Nm
c_1	constant	-0.04240011450454	-
c_2	constant	0.00000000029375	-
c_3	constant	0.03508217905067	-
c_4	constant	0.40662691102315	-
a	constant	0.00025724985785	-
p	constant	2.09945271667129	-

where $\mathbf{f}(\mathbf{x})$ and $\mathbf{g}(\mathbf{x})$ are the nominal functions.

Taking into account the deviations from the nominal condition and the noise in the measured parameters, the slip dynamics becomes:

$$\dot{\lambda} = [\mathbf{f}(\mathbf{x}) + \Delta\mathbf{f}(\mathbf{x})] + [\mathbf{g}(\mathbf{x}) + \Delta\mathbf{g}(\mathbf{x})] [\mathbf{u} + n(x)] \qquad (4.2)$$

where the uncertainties are represented by $\Delta\mathbf{f}(\mathbf{x})$ and $\Delta\mathbf{g}(\mathbf{x})$, while $n(x)$ is the noise in the measured parameters. Therefore, the robustness of a standard feedback linearization cannot be guaranteed, due to uncertainties. In order to ensure the robustness of the controller, a neural network model is employed and trained to estimate the non-linear system and due to its adaptation capability, it will behave well under varying conditions.

Neural networks have been shown to approximate arbitrary non-linear functions quite well (Yeşildirek and Lewis, 2001; Lin and Hsu, 2003; Hsu et al., 2008; Poursamad, 2009) and the NNFBL control method is known for its fast and accurate mapping capability (Akbarimajd and Kia, 2010). Two steps are involved in the indirect adaptive controller design, using neural networks: system identification and controller design. These are presented in the sections that follow.

4.1 System Identification

The *system identification* process involves collecting a set of training data through experiments. This is achieved through varying inputs to the system and observing the behaviour on the outputs. A set of corresponding inputs and outputs data is then used to train the neural network to estimate the system's dynamics.

The system identification procedure is illustrated in Figure 4, where T_b is the input braking torque to both the ABS system and the neural network model, λ_p and λ_m are the ABS system's

and NN model's slip outputs respectively. The error signal is used for the training of the NN model to estimate the ABS system.
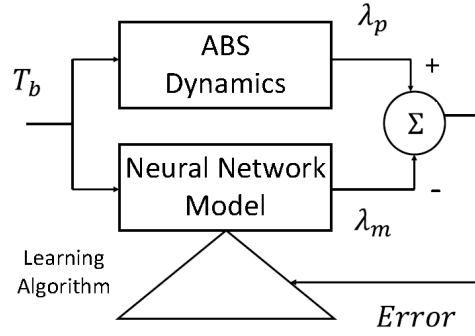

Figure 4: System identification of ABS dynamics for NNFBL control

The complete system identification process therefore involves: *Experimentation, Model structure selection, Model estimation* and *Model validation*

4.1.1 Experimentation

In the experimental stage, a set of input/output data is collected through experiments with the ABS model. It is important that the collected data covers the entire operating range of the ABS. To ensure that every dynamics of the plant are captured, the sampling time had to be smaller than the fastest dynamics.

The Simulink$^{\circledR}$ model of the experimental ABS rig shown in Figure 5 is used for data collection. The data set Z^n collected can be represented by Equation (4.3).

$$Z^n = f\{[u(k), y(k)]; k = 1, 2 \ldots, N\} \tag{4.3}$$

where $u(k)$ is the input to the system, which is the braking torque (T_b) and $y(k)$ the corresponding slip (λ) output. k is the number of the sample instant and the total number of samples taken is N (Pedro, Nyandoro and John, 2009). A total of 300 samples are collected at a sampling rate of $T_s = 0.01 sec$. The braking torque is a random input with a maximum value of $8Nm$ and a minimum value of 0. The output slip value is limited to the maximum value of 0.4, which is the peak value for the two contacting wheels and a minimum value of 0.

4.1.2 Model structure selection

Based on the slip dynamics developed in Section 2 and given by Equation (2.7), the structure of the NN model to be selected, should be able to estimate the functions $f(\cdot)$ and $g(\cdot)$. Therefore the *Non-linear Autoregressive-Moving Average* model is selected for this work, which is presented in its discrete form as (Pedro et al., 2009; Akbarimajd and Kia, 2010):

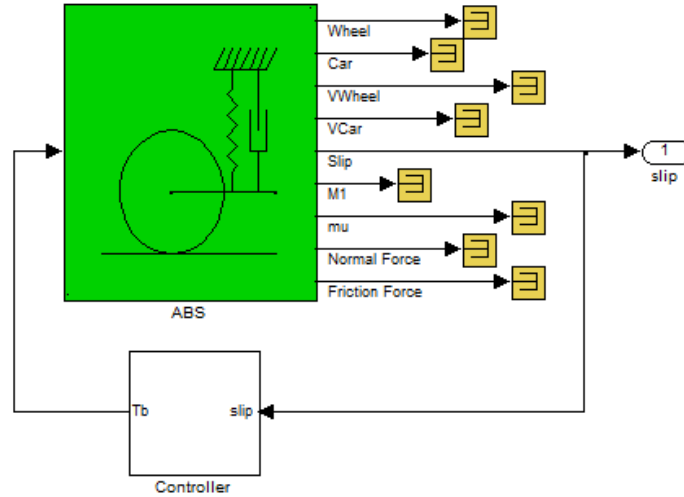$$y(k + d) = F[y(k), y(k - 1), \ldots, y(k - na + 1), u(k), u(k - 1), \ldots, u(k - nb + 1)] \tag{4.4}$$

Figure 5: ABS rig Simulink$^{\circledR}$ model

where $F(\cdot)$ is a non-linear function, na is the number of past outputs, nb is the number of past inputs, and d is the system delay. The network is trained during identification to approximate the non-linear function $F(\cdot)$. By Taylor series expansion of $F(\cdot)$, Equation (4.4) becomes (Akbarimajd and Kia, 2010):

$$
\begin{aligned}
y(k+d) = \; & f[y(k), y(k-1), \ldots, y(k-na+1), u(k-1), \ldots, u(k-nb+1)] \\
& + g[y(k), y(k-1), \ldots, y(k-na+1), u(k-1), \ldots, u(k-nb+1)] \cdot u(k) \quad \text{(4.5)}
\end{aligned}
$$

Equation (4.5) has elements similar to the ABS system dynamics presented in Equation (4.1). NNFBL operates on the same principles like the standard FBL, in which the goal is to cancel the non-linearity in the system to generate a linear system. This is achieved by training two *Multi-layered perceptron* (MLP) neural networks to approximate the non-linear functions $f(\cdot)$ and $g(\cdot)$ as:

$$
\begin{aligned}
\hat{y}(k+d) = \; & \hat{f}[y(k), y(k-1), \ldots, y(k-na+1), u(k-1), \ldots, u(k-nb+1)] \\
& + \hat{g}[y(k), y(k-1), \ldots, y(k-na+1), u(k-1), \ldots, u(k-nb+1)] \cdot u(k) \quad \text{(4.6)}
\end{aligned}
$$

where $\hat{f}(\cdot)$ and $\hat{g}(\cdot)$ are used as approximates for the $f(\cdot)$ and $g(\cdot)$ non-linear functions. The design objective of the controller therefore, is to ensure the system output follows a reference trajectory based on Equation (4.5).

$$
u(k) = \frac{y_r(k+d) - \hat{f}[y(k), \ldots, y(k-n+1), u(k-1), \ldots, u(k-n+1)]}{\hat{g}[y(k), \ldots, y(k-n+1), u(k-1), \ldots, u(k-n+1)]} \quad \text{(4.7)}
$$

However, the control law given by Equation (4.7) is not feasible, because to compute $u(k)$, $y(k)$ is required. Therefore if the plant delay is chosen to be $d \geq 2$ with model order of $n = na =$

$nb = 2$, the following practical NNFBL control law will be realised (Norgaard, 2000; Akbarimajd and Kia, 2010):

$$u(k) = \frac{y_r(k+d) - \hat{f}[y(k), \ldots, y(k-n+1), u(k), \ldots, u(k-n+1)]}{\hat{g}[y(k), \ldots, y(k-n+1), u(k), \ldots, u(k-n+1)]} \tag{4.8}$$

4.1.3 Multi-layered perceptron approximator

The *multi-layered perceptron* (MLP) network is employed for this work; it is known to be good at learning dynamics of non-linear systems (Norgaard et al., 2003). According to (Hagan, Demuth and De-Jesus, 2002) and (Hornik, Stinchcombe and White, 1989), a two-layer network with sigmoid transfer function in the hidden layer and linear transfer function in the output layer can be regarded as a universal function approximator . They are also known for their robustness, and the availability of fast training algorithms. In addition, the MLP responses fast in re-call mode, as it does not have to carry out any further iterations (Bruckner and Rudolph, 2000; Norgaard et al., 2003).

A schematic representation of a typical MLP with three layered neural network, made-up of an input layer, an output layer and one hidden layer is shown in Figure 6.
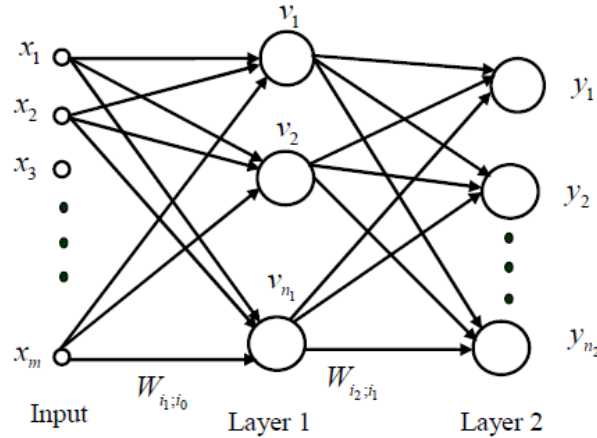

Figure 6: Three-layered neural network structure

Through the process of *training*, the adjustable weights (W_{ij}), are determined from a set of *training data* (x_i) collected during the *experimentation* stage. Using the MLP shown in Figure 6, the predicted output $(\hat{y})$ is given by:

$$\hat{y}(t, \theta) = V_i \left[\sum_{j=1}^{q} W_{ij} h_j(\mathbf{w}) + W_{i0} \right] \tag{4.9}$$

where V_i is the activation function, h_i is the input to the hidden layer. If the training set is given by Equation (4.3); the goal is to determine a mapping from the training data set to possible weights, i.e. $Z^n \to \hat{\theta}$ so that the network predicts $\hat{y}(t)$ as close as possible to the system's output $y(t)$. The prediction error is based on the mean square error criterion (MSE). The *sigmoid*

activation function v_i is used in the hidden layer, and is given by Equation 4.10.

$$v_{i_2} = \frac{1}{1 + e^{-h_{i_1}}}$$ (4.10)

where h_{i_1} is given by:

$$h_{i_1} = \sum_{i_1=0}^{m} W_{i_1 i_0} x_{i_0}$$ (4.11)

The back-propagation (BP) algorithm is employed to adjust the neural networks weights aimed at minimizing the cost function given by Equation (4.12). This learning method has a fast convergent rate (Norgaard et al., 2003; Behera and Kar, 2009) and it is recommended for most control applications and real-time implementations (Behera and Kar, 2009).

$$E_{i_2} = \frac{1}{n} \sum_{i=1}^{n} \left(y_{d_{i_2}}(t) - y_{i_2}(t) \right)^2$$ (4.12)

where $y_{d_{i_2}}(t)$ is the desired response and y_{i_2} is the model output of the i_2^{th} unit of the output layer and n is the number of training samples.

In the experimental phase, 300 data-set is generated, this is divided into three portions. 50% of the data is used for the training of the neural network model, 25% is used for testing the trained NN model and the remaining 25% is used for the validation.

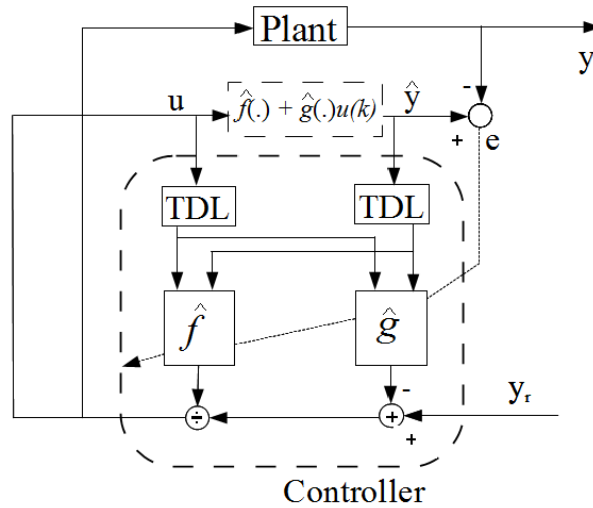The closed-loop block diagram of the NNFBL controller is shown in Figure 7

Figure 7: Block diagram of NNFBL controller

The NARMA-L2 toolbox in Matlab® / Simulink® is employed for the system identification. The structure of the neural network model, the parameters used for the neural network identification process and their numerical values are presented in Table 2. A sampling time of $0.01sec$ is used to conform with the micro-controller sampling time of the experimental rig. With this restriction, the results obtained are presented in Table 3.

Table 2: System identification parameters and their numerical values

Parameters	Values
Number of layers	2
Number of hidden layer neurons	9
number of past outputs (na)	2
Number of past inputs (nb)	2
Number of iterations	500
Training algorithm	Levenberg-Marquardt
Sampling time	0.01 sec
Maximum plant input	8 Nm
Minimum plant input	0 Nm
Maximum plant output	0.4
Minimum plant output	0

Table 3: Result of system identification

Parameters	Results
Performance (mse)	1.99×10^{-6}
Number of epoch	6

5 Experimental Procedure and Results

For the purpose of comparative analysis, a PID controller is implemented as a benchmark controller. The PID controller is commonly used in industry (O'Dwyer, 2009) and it has been successfully applied to wheel slip control (Yoo, 2006; Jiang and Gao, 2001). The PID controller structure used for the experiments is given by Equation (5.1),

$$U(s) = \left[K_p \left(\frac{T_i s + 1}{T_i s} \frac{T_d s + 1}{\Psi T_d s + 1} \right) \right] E(s) \tag{5.1}$$

where $E(s)$ and $U(s)$ are the error signal and plant input signal respectively, K_p is the proportional gain, T_d is the derivative time constant, T_i is the integral step-time and Ψ is the lag factor in the derivative component of the PID.

The selection of the PID gains is carried out using the Simulink$^{®}$ optimization toolbox. The plant output is constrained to a slip value of 0.18 and a gradient descent method with a tolerance of 0.001 is used to search the optimal gains. The iterations are limited to 100, but the system stabilizes after 70 iterations. The gains are presented in Table 4.

5.1 Experimental Procedure

For each test run, the wheels are accelerated to a speed of approximately $68 km/h$. Once the required speed is achieved, the braking process commenced. A fixed step size of $10 ms$ is used for the experiments, which is the recommended value for the current experimental set-up (Manual, 2009) along with the fifth-order integration method. At the end of each test-run the

Table 4: PID gains for ABS rig

Parameter	Gain
K_p	5
T_i	0.198223
T_d	1
Ψ	0.3

data for the vehicle and wheel deceleration, applied torque, slip tracking and the stopping distances are logged to the workspace for plotting.

The current set-up do not provide the means of testing the controller on different road conditions (Topalov, Oniz, Kayacan and Kaynak, 2011). Hence, experiments were conducted for a case of slip regulation at a desired slip value of $\lambda_d = 0.2$ and a case of slip tracking, in which the slip trajectory was varied from 0 to 0.3 to evaluate the slip tracking performance of the proposed controller, thereby imitating changes in road condition.

5.2 Experimental Results and Discussions

Figure 8 shows comparative plots for the case of constant slip regulation at a desired slip of $\lambda = 0.2$. Figure 9 is the slip plots for the case of slip tracking from an initial slip of zero to a final slip value of $\lambda = 0.3$. Figures 10 to 13 present the vehicle and wheel deceleration plots for the PID controller and the proposed NNFBL for regulation and tracking scenarios. The braking torque plots are shown in Figures 14 and 15 for regulation and tracking scenarios respectively.
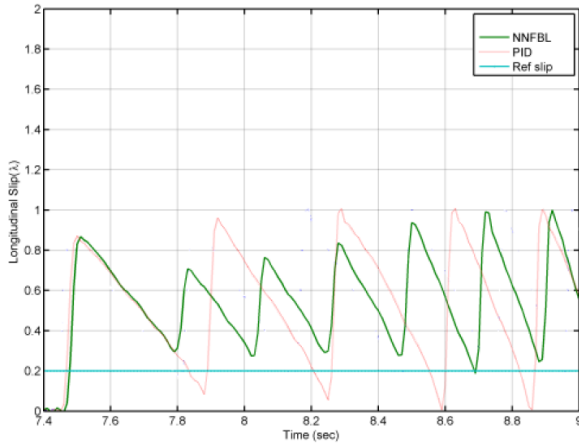

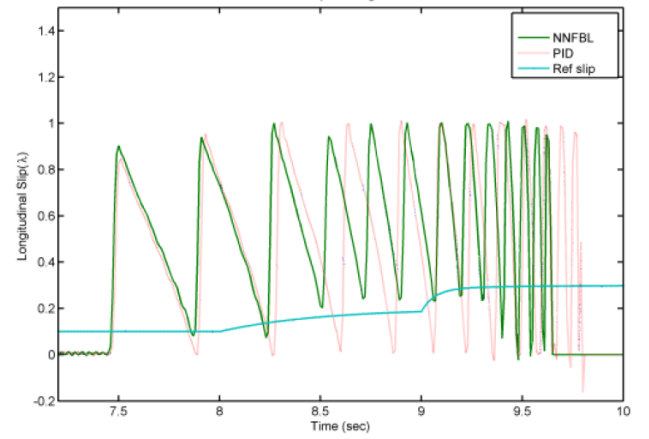Figure 8: Experimental results for slip regulation at $\lambda = 0.2$

Figure 9: Experimental results for slip tracking of $\lambda = 0$ to 0.2

Three performance indices are used for the evaluation of the effectiveness of the controllers. The summary of the performance indices for the controllers for the case of slip regulation and slip tracking are presented in Tables 5 and 6 respectively for the hardware-in-the-loop (HiL) experiments. A small index value is an indication of a good performance.
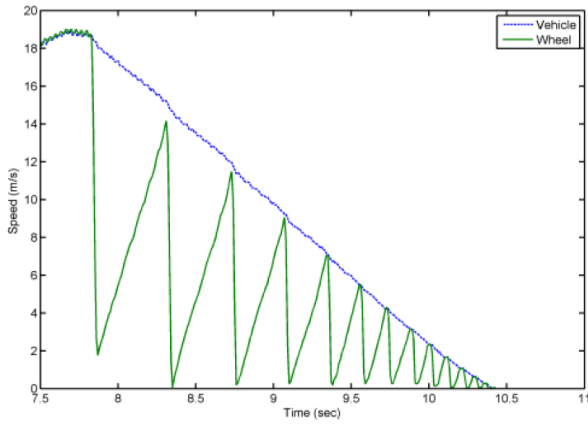
Figure 10: Experimental results for deceleration of vehicle and wheel using PID controller for the case of slip regulation
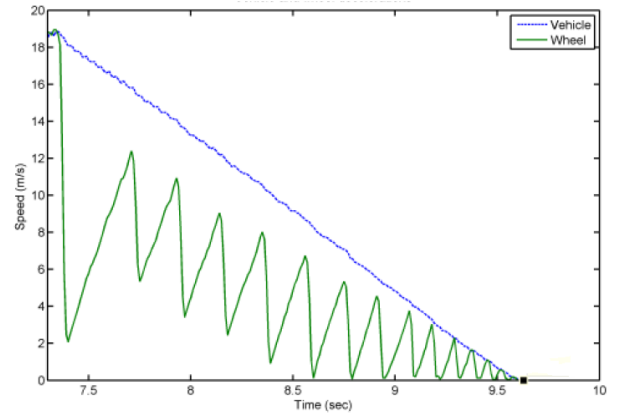

Figure 11: Experimental results for deceleration of vehicle and wheel using NNFBL controller for the case of slip regulation
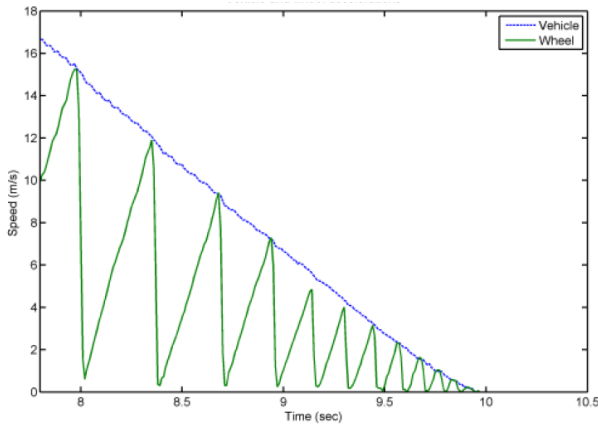

Figure 12: Experimental results for deceleration of vehicle and wheel using PID controller for the case of slip tracking
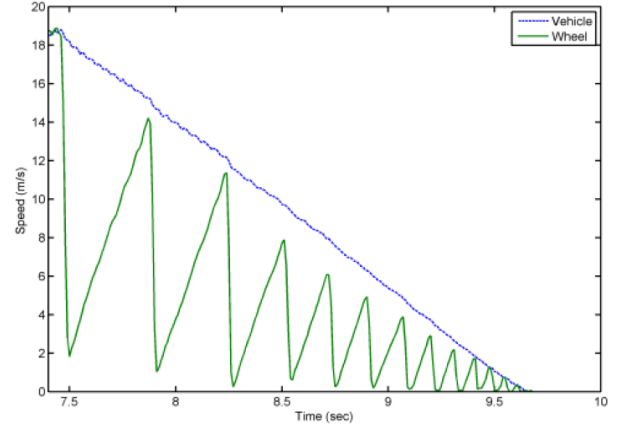

Figure 13: Experimental results for deceleration of vehicle and wheel using NNFBL controller for the case of slip tracking

Considering the plots of the slip regulation, the PID controller exhibits higher slip values than the NNFBL controller, before the end of the experiment. The NNFBL records high slip values only towards the end of the experiment, reaching its maximum peak value as expected in reality. The NNFBL recorded the lowest effective braking torque of $39Nm$ compared to the $108Nm$ by the PID controller as indicated in Table 5. The results of the deceleration of the vehicle and wheel show the NNFBL performed better than the PID by recording the lowest stopping distance of $20.75m$ as against $22.17m$ by the PID controller.

Considering the plots of the slip tracking case, a reference slip trajectory is imposed. This is done to imitate changes in road condition, thereby evaluating the robustness of the controllers. Similar to the case of slip regulation, braking commenced at an initial longitudinal velocity of $68km/h$ $(1500rpm)$ until *rest*. There was no further tuning of the controllers so that the robustness of the controllers could be evaluated. From the experimental plots (Figure 9)
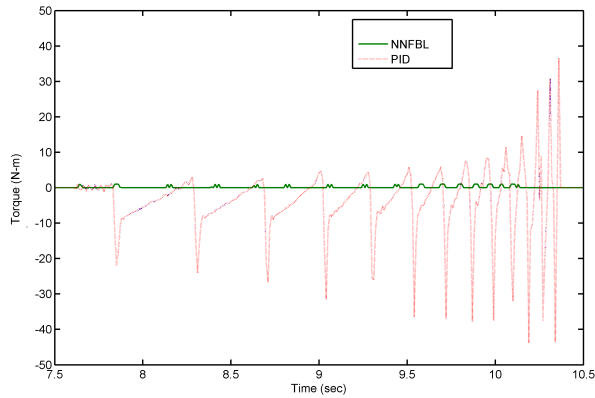
Figure 14: Experimental results for braking torques for for the case of slip regulation
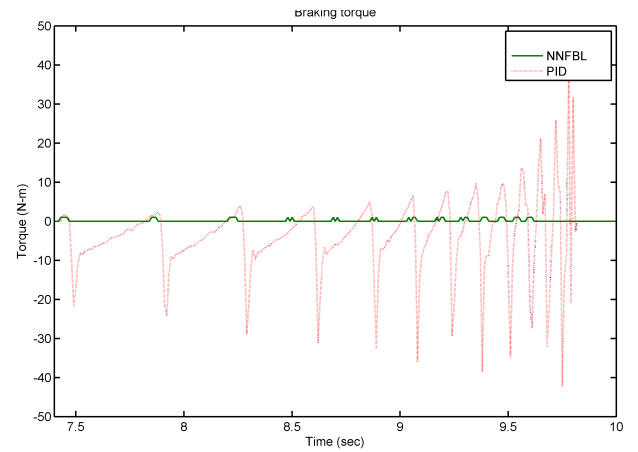

Figure 15: Experimental results for braking torques for for the case of slip tracking

Table 5: Performance indices for case of slip regulation from HiL experiments

Performance index	PID	NNFBL
Slip regulation - $\int_{0}^{t_f} (\lambda - \lambda_d)^2 dt$	0.7951	0.7356
Braking torque - $\int_{0}^{t_f} T_b^2 dt \ ((Nm)^2)$	108.5	39.15
Stopping distance - $\int_{0}^{t_f} v dt \ (m)$	22.17	20.75

the two controllers exhibit high slip values, indicating locking of wheel for short time periods. Using the slip performance index (Table 6), however, reveals the PID to perform better than the NNFBL. Observing the effective braking torque plots, the NNFBL has the best index, this implies that the PID controller achieved good slip tracking at a higher cost of the braking torque.

The deceleration of the vehicle and wheel reveals the NNFBL to have recorded a slightly shorter stopping distance, which is $21.32m$ as against $22.15m$ recorded by the PID controller.

Table 6: Performance indices for case of slip tracking from HiL experiments

Performance index	PID	NNFBL
Slip tracking - $\int_{0}^{t_f} (\lambda - \lambda_d)^2 dt$	0.6397	0.6457
Braking torque - $\int_{0}^{t_f} T_b^2 dt \ ((Nm)^2)$	137.97	40.36
Stopping distance - $\int_{0}^{t_f} v dt \ (m)$	22.15	21.32

6 Conclusion and Future Work

This work proposes a neural network-based input-output feedback linearization slip control for anti-lock braking systems. Experimental results generated from a laboratory anti-lock braking system test rig are presented. A comparative analysis of the proposed controller against the performance of a PID controller is presented. The NNFBL controller exhibits good performances with respect to the slip regulation, it achieved relatively shorter stopping distances and exhibits good convergence of slip tracking. The results obtained from this work, reveal that slip regulation using neural network based controllers is feasible for different optimum slip values, and is robust to external disturbances. Hence, it is concluded that the proposed NNFBL solution demonstrates potential for implementation.

The proposed controller was tested on a laboratory test rig with the aim of correlating theory with practice, and not aimed at producing a prototype. Hence limited test runs were conducted and full evaluation of the controllers on a real vehicle was not carried out. A simple straight line braking was considered as the laboratory equipment can only be used for such an operation. However, a braking and cornering manoeuvre would be an interesting aspect to be investigated. Future work will involve testing of the ABS controller on an actual vehicle.

References

Adaryani, M. R. and Afrakhte, H. 2011. NARMA-L2 controller for three-area load frequency control, *Proceedings of the 19th Iranian IEEE Conference on Electrical Engineering (ICEE), Tehran, Iran*, pp. 1 –6.

Akbarimajd, A. and Kia, S. 2010. NARMA-L2 controller for 2-DoF underactuated planar manipulator, *Proceedings of the 11th International Conference on Control, Automation, Robotics and Vision, Singapore*, pp. 195 – 200.

Awwad, A., Abu-Rub, H. and Toliyat, H. 2008. Nonlinear autoregressive moving average (NARMA-L2) controller for advanced ac motor control, *Proceedings of the 34th IEEE Conference on Industrial Electronics, IECON 2008, Orlando, Florida, USA*, pp. 1287 –1292.

Bakker, E., Pacejka, H. and Lidner, L. 1989. A new tire model with an application in vehicle dynamics studies, *SAE Technical Series* (890087): 83 – 95.

Behera, L. and Kar, I. 2009. *Intelligent Systems and Control Principles and Applications*, Oxford University Press, India.

Bruckner, S. and Rudolph, S. 2000. Neural networks applied to smart structure control, *Proceedings of SPIE, San Jose, CA, USA*, Vol. 4055, p. 288.

Chikhi, F., El Hadri, A. and Cadiou, J. 2005. ABS control design based on wheel-slip peak localization, *Proceedings of the Fifth International Workshop on Robot Motion and Control RoMoCo2005, Dymaczewo, Poland*, pp. 73 – 77.

Corno, M., Savaresi, S. M. and Balas, G. J. 2009. On linear-parameter-varying (LPV) slip-controller design for two-wheeled vehicles, *International Journal of Robust and Nonlinear Control* **19**(12): 1313–1336.

Hagan, M. T., Demuth, H. B. and De-Jesus, O. 2002. An introduction to the use of neural networks in control systems, *International Journal of Robust and Nonlinear Control* **12**: 959–985.

Hornik, K. M., Stinchcombe, M. and White, H. 1989. Multilayer feedforward networks are universal approximators, *Journal of Neural Networks* **2**: 359 – 366.

Hsu, C.-F., Lee, T.-T., Hsu, C.-Y. and Lin, C.-M. 2008. Neurocontroller design and stability analysis for antilock braking systems, *Proceedings of the IEEE International Conference on Systems, Man and Cybernetics (SMC)*, pp. 3388 –3393.

Jiang, F. and Gao, Z. 2001. An application of nonlinear PID control to a class of truck ABS problems, *Proceedings of the 40th IEEE Conference on Decision and Control, Orlando, Florida, USA*, Vol. 1, pp. 516 –521.

Lidner, L. 1993. Experience with the magic formula tyre model, *in* H. B. Pacejka (ed.), *Proceedings of 1st International Colloquium on Tyre Models for Vehicle Dynamics Analysis (Supplement to Vehicle System Dynamics)*, Vol. 21, SWETS & ZEITLINGER B.V. AMSTERDAM / LISSE, pp. 30– 46.

Lin, C.-M. and Hsu, C.-F. 2003. Neural-network hybrid control for antilock braking systems, *IEEE Transactions on Neural Networks* **14**(2): 351 – 359.

Lin, J.-S. and Ting, W.-E. 2007. Nonlinear control design of anti-lock braking systems with assistance of active suspension, *Control Theory Applications, IET* **1**(1): 343 –348.

Manual, I. U. 2009. *The laboratory antilock braking system controlled from PC Technical Report*, Inteco Ltd., Poland.

Mirzaei, A., Moallem, M., Dehkordi, B. and Fahimi, B. 2006. Design of an optimal fuzzy controller for antilock braking systems, *IEEE Transactions on Vehicular Technology* **55**(6): 1725 –1730.

Norgaard, M. 2000. Neural network based system identification toolbox, *Technical report*, Department of Automation, Technical University of Denmark.

Norgaard, M., Ravn, O., Poulsen, N. and Hansen, L. 2003. *Neural Networks for Modelling and Control of Dynamic Systems: A Practitioner's Handbook*, Springer-Verlag, London.

O'Dwyer, A. 2009. *Handbook of PI and PID Controller Tuning Rules*, 3rd edn, Imperial College Press, London.

Oosten, J. V. and Bakker, E. 1993. Determination of magic tyre model parameters, *in* H. B. Pacejka (ed.), *Proceedings of 1st International Colloquium on Tyre Models for Vehicle Dynamics Analysis (Supplement to Vehicle System Dynamics Vol. 21)*, Vol. 21, SWETS & ZEITLINGER B.V. AMSTERDAM / LISSE, pp. 19–29.

Pacejka, H. and Bakker, E. 1993. The magic formula tyre model, *in* H. B. Pacejka (ed.), *Proceedings of 1st International Colloquium on Tyre Models for Vehicle Dynamics Analysis (Supplement to Vehicle System Dynamics Vol. 21)*, Vol. 21, SWETS & ZEITLINGER B.V. AMSTERDAM / LISSE, pp. 1–18.

Park, K.-S. and Lim, J.-T. 2008. Wheel slip control for ABS with time delay input using feedback linearization and adaptive sliding mode control, *Proceedings of the International Conference on Control, Automation and Systems (ICCAS), Seoul, Korea*, pp. 290 –295.

Pedro, J., Nyandoro, O. and John, S. 2009. Neural network based feedback linearisation slip control of an anti-lock braking system, *Proceedings of the 7th Asian Control Conference (ASCC)*, pp. 1251 –1257.

Poursamad, A. 2009. Adaptive feedback linearization control of antilock braking systems using neural networks, *Mechatronics* **19**(5): 767 − 773.

Precup, R. E., Spataru, S., Petriu, E. M., Preitl, S., Radac, M.-B. and Dragos, C.-A. 2010. Stable and optimal fuzzy control of a laboratory antilock braking system, *Proceedings of the IEEE/ASME International Conference on Advanced Intelligent Mechatronics (AIM), Montreal, Canada*, pp. 593 –598.

Shin, H.-S., Choi, H.-L. and Lim, J.-T. 2006. Feedback linearisation of uncertain nonlinear systems with time delay, *IEE Proceedings on Control Theory and Applications* **153**(6): 732 –736.

Topalov, A. V., Oniz, Y., Kayacan, E. and Kaynak, O. 2011. Neuro-fuzzy control of antilock braking system using sliding mode incremental learning algorithm, *Neurocomputing* **74**(11): 1883 − 1893.

Vassileiou, A., Maris, F., Kitikidou, K. and Angelidis, P. 2012. Artifical neural networks for improved predictions in flow estimation, *International Journal of Artificial Intellgence* **9**(A12): 186 − 201.

Wang, H., Tanaka, K. and Griffin, M. 1995. Parallel distributed compensation of nonlinear systems by takagi-sugeno fuzzy model, *Proceedings of the 4th International Joint Conference on Fuzzy Systems, Yokohama, Japan*, Vol. 2, pp. 531 –538 vol.2.

Xu, C., Cheng, K., Sha, L., Ting, W. and Ding, K. 2009. Simulation of the integrated controller of the anti-lock braking system, *Proceedings of the 3rd International Conference on Power Electronics Systems and Applications, Hong Kong*, pp. 1 –3.

Yeşildirek, A. and Lewis, F. L. 2001. Adaptive feedback linearization using efficient neural networks, *J. Intell. Robotics Syst.* **31**: 253–281.

Yoo, D. 2006. *Model based wheel slip control via constrained optimal algorithm*, Master's thesis, RMIT University, Melbourne, Australia.

Yu, F., Feng, J. and Li, J. 2002. A fuzzy logic controller design for vehicle ABS with a on-line optimized target wheel slip ratio, *International Journal of Automotive Technology* **3**(4): 165 –170.

Zanten, A., Erhardt, R. and Lutz, A. 1990. Measurement and simulation of transients in longitudinal and lateral tire forces, *SAE Technical Series* **99**(900210): 300 –318.